DOI: 10.6060/ivkkt.20216407.6390

УДК: 537.525

ПАРАМЕТРЫ ПЛАЗМЫ И КОНЦЕНТРАЦИИ АКТИВНЫХ ЧАСТИЦ В СМЕСЯХ ФТОРУГЛЕРОДНЫХ ГАЗОВ С АРГОНОМ И КИСЛОРОДОМ

А.М. Ефремов, В.Б. Бетелин, К.А. Медников, K.-H. Kwon

Александр Михайлович Ефремов*

Ивановский государственный химико-технологический университет, Шереметевский просп., 7, Иваново, Российская Федерация, 153000
E-mail: amefremov@mail.ru*

Владимир Борисович Бетелин, Константин Александрович Медников

ФГУ ФНЦ НИИСИ РАН, Нахимовский просп., 36, к.1, Москва, Российская Федерация, 117218
E-mail: betelin@niisi.msk.ru, k.a.mednikov@gmail.com

Kwang-Ho Kwon

Korea University, 208 Seochang-Dong, Chochiwon, Korea, 339-800
E-mail: kwonkh@korea.ac.kr

Проведено сравнительное исследование электрофизических параметров плазмы и стационарного состава газовой фазы в плазме индукционного ВЧ 13б56 МГц разряда в смесях $CF_4 + O_2 + Ar$, $CHF_3 + O_2 + Ar$ и $C_4F_8 + O_2 + Ar$. В качестве постоянных внешних параметров выступали доля фторуглеродного компонента (50%), общее давление газа (6 мтор), вкладываемая мощность (700 Вт) и мощность смещения (200 Вт). Схема исследования включала диагностику плазмы зондами Лангмюра и 0-мерное (глобальное) моделирование кинетики плазмохимических процессов. Найдено, что полимеризационная способность бескислородных (50% Ar) и кислородсодержащих (50% O_2) смесей согласуется с отношением z/x в исходной молекуле $C_xH_yF_z$. Замещение аргона на кислород приводит к однотипным изменениям параметров электронной и ионной компонент плазмы (температуры электронов, концентраций заряженных частиц и энергии ионной бомбардировки), всегда снижает концентрации полимеробразующих радикалов и толщину полимерной пленки, но оказывает различное влияние на кинетику атомов фтора. Увеличение доли кислорода в смесях 50% $CF_4 + O_2 + Ar$ и 50% $CHF_3 + O_2 + Ar$ приводит к монотонному росту концентрации атомов фтора. Механизмы этих явлений связаны с увеличением скорости генерации атомов и снижением частоты их гибели, соответственно. Добавление кислорода в системе 50% $C_4F_8 + O_2 + Ar$ снижает скорость генерации атомов фтора, но не приводит к заметным изменениям частот их гибели. Это соответствует монотонному снижению концентрации атомов фтора при увеличении содержания кислорода в смеси. В результате, стационарная концентрация атомов фтора в условиях 50% O_2 увеличивается в ряду C_4F_8 - CHF_3 - CF_4.

Ключевые слова: фторуглеродные газы, плазма, параметры, активные частицы, ионизация, диссоциация, травление, полимеризация

Для цитирования:
Ефремов А.М., Бетелин В.Б., Медников К.А., Kwon K.-H. Параметры плазмы и концентрации активных частиц в смесях фторуглеродных газов с аргоном и кислородом. *Изв. вузов. Химия и хим. технология*. 2021. Т. 64. Вып. 7. С. 46–53

For citation:
Efremov A.M., Betelin V.B., Mednikov K.A., Kwon K.-H. Plasma parameters and densities of active species in mixtures of fluorocarbon gases with argon and oxygen. *ChemChemTech* [*Izv. Vyssh. Uchebn. Zaved. Khim. Khim. Tekhnol.*]. 2021. V. 64. N 7. P. 46–53

PLASMA PARAMETERS AND DENSITIES OF ACTIVE SPECIES IN MIXTURES OF FLUOROCARBON GASES WITH ARGON AND OXYGEN

A.M. Efremov, V.B. Betelin, K.A. Mednikov, K.-H. Kwon

Alexander M. Efremov*

Ivanovo State University of Chemistry and Technology, Sheremetevskiy ave., 7, Ivanovo, 153000, Russia
E-mail: efremov@isuct.ru *

Vladimir B. Betelin, Konstantin A. Mednikov

SRISA RAS, Nakhimovsky ave., 36, bld. 1, Moscow, 117218, Russia
E-mail: betelin@niisi.msk.ru, k.a.mednikov@gmail.com

Kwang-Ho Kwon

Korea University, 208 Seochang-Dong, Chochiwon, Korea, 339-800
E-mail: kwonkh@korea.ac.kr

The comparative study of plasma electro-physical parameters and steady-state gas phase compositions in $CF_4 + O_2 + Ar$, $CHF_3 + O_2 + Ar$ and $C_4F_8 + O_2 + Ar$ gas mixtures was carried out under the condition of 13.56 MHz inductive RF discharge. Constant processing parameters were fluorocarbon component fraction in a feed gas (50%), total gas pressure (6 mTorr), input power (700 W) and bias power (200 W). The investigation scheme included plasma diagnostics by Langmuir probes and 0-dimensional (global) modeling of plasma chemistry. It was found that polymerizing ability in both non-oxygenated (50% Ar) and oxygenated (50% O_2) gas systems correlates with the x/z ratio in the original $C_xH_yF_z$ molecule. The substitution of Ar for O_2 causes similar changes in electrons- and ions-related plasma parameters (electron temperature, plasma density, ion bombardment energy), always suppresses densities of polymerizing radicals and polymer film thickness, but has the different impact on the F atom kinetics. An increase in O_2 fraction in 50% $CF_4 + O_2 + Ar$ and 50% $CHF_3 + O_2 + Ar$ gas mixtures results in monotonically increasing F atom densities. Mechanisms of these phenomena are increasing F atom formation rate and decreasing the F atom decay frequency, respectively. The addition of oxygen to 50% $C_4F_8 + O_2 + Ar$ gas mixture lowers the F atom formation rate, but does not result in sufficient changes in their decay frequency. This corresponds to monotonically decreasing F atom density toward O_2-rich plasmas. As a result, the steady-state density of F atoms in gas systems with 50% O_2 increases in the sequence of C_4F_8 - CHF_3 - CF_4.

Key words: fluorocarbon gases, plasma, parameters, active species, ionization, dissociation, etching, polymerization

INTRODUCTION

Fluorocarbon gases with a general formula of $C_xH_yF_z$ are frequently used for the reactive-ion etching (RIE) of silicon and silicon-based materials [1-3]. This process represents the critical part of the photolithography circle because it determines patterning quality and thus, whole device dimension and performance. Among the fluorocarbon gas family, the CF_4 is characterized by the highest z/x ratio and provides the domination of etching over the surface polymerization process under the typical RIE conditions [4]. This allows one to obtain high absolute etching rates, but results in both nearly isotropic etching profiles for Si (due to the spontaneous chemical reaction between silicon and fluorine atoms) and low SiO_2/Si selectivity [3, 4]. Oppositely, more polymerizing fluorocarbons with $z/x < 3$ (for example, CHF_3 and C_4F_8) allow one to obtain the anisotropic high aspect ratio etching of Si (due to the passivation of side walls by the fluorocarbon polymer film [2, 4]) as well as provide the much higher etching selectivity over the SiO_2 (due to the much lower polymer film thickness on the oxygen-containing surface [4]). At the same time, the negative issues are the decrease in absolute Si and SiO_2 etching rates and an increase in etching residues. It is known also that all fluorocarbons are frequently combined with Ar or O_2 with the aims of accelerating the physical etching pathway, increasing the F atoms yield and suppressing surface polymerization [2, 3]. Therefore, the choice of an appropriate fluorocarbon gas, additive components and their mixing ratios is a powerful tool to adjust output characteristics of RIE process for a given type of etched material. The mandatory condition for the use

of this tool is the understanding of relationships between processing conditions, internal plasma parameters and steady-state densities of plasma active species.

Until now, there were many works dealt with investigations of plasma parameters and gas-phase compositions in CF_4 + Ar/O_2 [5-8, 10], CHF_3 + Ar/O_2 [9-11] and C_4F_8 + Ar/O_2 [7, 12-15] plasmas. In fact, results of these researches allowed one a) to figure out key gas-phase processes determining kinetics of fluorine atoms and polymerizing radicals; b) to compose kinetic schemes (sets of reactions with corresponding rate coefficients) for the adequate description of plasma chemistry in the presence of oxygen; and c) to understand basic responses of both etching and polymerization kinetics to changes in processing parameters (input power, pressure and gas mixing ratios). In addition, our previous studies [8, 11, 14-16] suggested an advanced research scheme as a combination of etching experiments, plasma diagnostics by Langmuir probes and plasma modeling. Such a method clearly demonstrates how processing parameters do effect on gas-phase plasma characteristics as well as allows one to analyze etching mechanisms with model-predicted fluxes of plasma active species. The problem is that the most of existing data for various gas chemistries were obtained at different processing conditions and/or in different types of plasma reactors. As such, in many cases it is impossible to compare directly the features of gas-phase plasma characteristics even for widely used fluorocarbon-based gas mixtures and thus, to evaluate their etching performances in respect to the given treated material. Such situation retards both optimization of reactive-ion etching technologies and the overall progress in the electronic device fabrication field.

The idea of this work was to carry out the comparative study of plasma electro-physical parameters and steady-state gas phase compositions in CF_4 + O_2 + Ar, CHF_3 + O_2 + Ar and C_4F_8 + O_2 + Ar gas mixtures under one and the same operating conditions. Corresponding fluorocarbon gases provide a continuous decrease of z/x ratio in the sequence of CF_4 – CHF_3 – C_4F_8 that causes sufficient differences in their polymerizing abilities and fluorine atom densities [16]. Accordingly, the main goals were 1) to compare how the change in O_2/Ar mixing ratio does influence electrons- and ions related plasma parameters; 2) to analyze differences in densities of fluorine atoms and polymerizing radicals in the presence of oxygen; and 3) to suggest features of etching and polymerization kinetics based on gas-phase plasma characteristics.

EXPERIMENTAL AND MODELING DETAILS

Experiments were performed in the planar (with top-side flat coil) inductively coupled plasma (ICP) reactor described in our previous works [14-16]. Plasma was excited using the 13.56 MHz power supply while another 12.56 MHz rf generator biased the bottom electrode. The latter allowed one to adjust the ion bombardment energy through the negative dc bias voltage ($-U_{dc}$). An actual $-U_{dc}$ value was measured by high-voltage probe (AMN-CTR, Youngsin Eng.). Constant processing parameters were total gas flow rate (q = 40 sccm), gas pressure (p = 6 mTorr), input power (W_{inp} = 700 W) and bias power (W_{dc} = 200 W). The variable parameter was the O_2/Ar mixing ratio in CF_4 + O_2 + Ar, CHF_3 + + O_2 + Ar and C_4F_8 + O_2 + Ar gas mixtures with fixed 50% fraction of fluorocarbon component. Accordingly, an increase in O_2 fraction in a feed gas, $y(O_2)$, from 0-50% corresponded to the full substitution of Ar for O_2.

In order to obtain the data on electro-physical plasma parameters, such as electron temperature (T_e) and ion current density (J_+), we used plasma diagnostics by the double Langmuir probe (DLP2000, Plasmart Inc.). The probe installation and measurement details have been described in Refs. [8, 11]. The treatment of raw I-V curves was based on well-known statements of the double probe theory for low pressure plasmas [17].

In order to analyze the influence of O_2/Ar mixing ratio on kinetics and densities of plasma active species, we used a simplified 0-dimensional (global) model. Detailed information on model assumptions and algorithm may be found in Refs. [7, 8, 15, 18]. Kinetic schemes (sets of chemical reactions with corresponding rate coefficients) were taken from published works that dealt with the modeling of CF_4 + Ar/O_2 [7, 8], CHF_3 + Ar/O_2 [11] and C_4F_8 + Ar/O_2 [7, 15] plasmas. As input parameters, the model used experimental data on T_e and J_+. The latter yielded the total density of positive ions n_+ as well as the electron density n_e assuming $n_e \approx n_+$. The low electronegativity of low pressure CF_4, CHF_3, C_4F_8 and O_2 plasmas has been confirmed in earlier works [5, 6, 9, 13, 19]. The neutral gas temperature (T_{gas}) was approximated by the typical (for given set of processing conditions, reactor type and geometry) value of ~ 600 K, as have been done in Refs. [10, 11, 14]. The output model parameters were volume-averaged steady-state densities of plasma active species and their fluxes to the etched surface.

RESULTS AND DISCUSSION

Features of electrons- and ions-related plasma parameters for CF_4 + Ar, CHF_3 + Ar and C_4F_8 + Ar

plasmas were subjects of detailed analysis in our previous studies [10, 14, 16, 18]. That is why the below discussion deals only with effects obtained during the substitution of argon for oxygen. Experiments indicated that the substitution of Ar for O_2 in all three gas mixtures causes similar changes in electron temperature, plasma density and negative dc bias voltage on the lower electrode (Table). Corresponding results may be briefly explained as follows:

- A decrease in T_e toward O_2-rich plasmas is caused by an increase in the electron energy loss due to increasing fraction of molecular components in a gas phase (Fig. 1). The reason is that the first excitation potential for Ar atom of ~ 11.6 eV (in fact, the starting point in the corresponding electron energy loss spectrum) is much higher than that for O_2 (~ 0.16 eV for the vibration excitation R1: $O_2(V=0) + e \rightarrow O_2(V>0) + e$). In addition, O_2 provides the low-threshold excitation of metastable states in R2: $O_2 + e \rightarrow O_2(a^1\Delta) + e$ ($\varepsilon_2 = 0.98$ eV) and R3: $O_2 + e \rightarrow O_2(b^1\Sigma) + e$ ($\varepsilon_3 = 1.64$ eV). As a result, the almost continuous energy loss spectrum from ~ 0.2 eV takes place.

- A decrease in plasma density with increasing O_2 content in a feed gas is provided by the simultaneous action of two mechanisms. These are a) decreasing ionization rate coefficients, according to the behavior of T_e (since $\varepsilon_{iz} \approx 12$-$15$ eV $> (3/2)T_e$ where ε_{iz} is the threshold energy for ionization, and $(3/2)T_e$ is the mean electron energy); and b) increasing densities of electronegative species due to both O_2 itself and oxygen-containing reaction products. The latter accelerates losses of positive ions and electrons through the ion-ion recombination and dissociative attachment, respectively. Ion current densities and ion fluxes follow the behavior of n_+ and also exhibit decreasing tendencies toward O_2-rich plasmas.

- An increase in negative dc bias is evidently connected with the decreasing ion flux. This is because the lower ion flux provides the weaker compensation for the excess negative charge produced by corresponding power supply under the condition of W_{dc} = const.

When analyzing kinetics of neutral species, it was found that all three gas mixtures exhibit sufficient dissimilarities in respect to fluorine atom kinetics. Such situation is provided by specific electron-impact dissociation mechanisms for original fluorocarbon molecules that pre-determine different first-step dissociation products and their interaction pathways with other species, including oxygen atoms and molecules.

In the CF_4 + Ar plasma, dominant fluorine-containing components are original CF_4 molecules, CF_3 radicals and F itself [5, 6, 18]. The formation of F atoms is mainly provided by R4: $CF_4 + e \rightarrow CF_3^+ + F + 2e$ and R5: $CF_x + e \rightarrow CF_{x-1} + F + e$ for x = 3, 4. The decay of atomic species is due to their heterogeneous recombination in R6: $F + F(s.) \rightarrow F_2$ and R7: $F + CF_x(s.) \rightarrow CF_{x+1}$, where index "(s.)" points out on the surface-bonded particle. The substitution of Ar for O_2 rapidly reduces densities of CF_x radicals (due to the decomposition of these species in R8: $CF_x + O/O(^1D) \rightarrow CF_{x-1}O + F$, R9: $CF_3 + CFO \rightarrow CF_4 + CO$ and R10: $CF_3 + CFO \rightarrow CF_2O + CF_2$), but introduces new formation pathways for F atoms. Among latters, most important are electron-impact reactions R11: $CFO + e \rightarrow CO + F + e$, R12: $CF_2O + e \rightarrow CFO + F + e$ and R13: $FO + e \rightarrow F + O + e$. High rate of R11 is provided by the fast formation of CFO species in R12 and R14: $CO + F \rightarrow CFO$ while the same effect for R12 is due to R10, R15: $2CFO \rightarrow CF_2O + CO$ and R16: $CFO + F \rightarrow CF_2O$. In addition, formation kinetics of fluorine atom in O_2-rich plasmas is noticeably affected by atom-molecular reactions R17: $FO + O/O(^1D) \rightarrow F + O_2$, R18: $2FO \rightarrow 2F + O_2$ and R19: $CFO + O \rightarrow CO_2 + F$. As a result, the substitution of Ar for O_2 leads to a continuous increase in the F atom formation rate and thus, the F atom density (Fig. 1(a)).

Table

Electrons- and ions-related plasma parameters in 50% $CF_4 + O_2$ + Ar, 50% $CHF_3 + O_2$ + Ar and 50% $C_4F_8 + O_2$ + Ar plasmas

Таблица. **Параметры электронной и ионной компоненты плазмы в смесях 50% $CF_4 + O_2$ + Ar, 50% $CHF_3 + O_2$ + Ar и 50% $C_4F_8 + O_2$ + Ar**

$y(O_2)$, %	$CF_4 + O_2$ + Ar			$CHF_3 + O_2$ + Ar			$C_4F_8 + O_2$ + Ar		
	T_e, eV	n_+, 10^{10} cm^{-3}	$-U_{dc}$, V	T_e, eV	n_+, 10^{10} cm^{-3}	$-U_{dc}$, V	T_e, eV	n_+, 10^{10} cm^{-3}	$-U_{dc}$, V
0	3.6	4.9	215	4.8	6.2	190	4.8	4.4	212
50	3.4	3.2	250	3.0	3.0	254	3.1	3.7	269

In the CHF_3 + Ar plasma, main fluorine-containing species are HF, CHF_3 and CF_x (x = 1-3) [9-11, 20]. The high density of HF [20, 21] is provided by two mechanisms, such as a) the direct formation of these species in R20: $CHF_3 + e \rightarrow HF + CF_2 + e$; and 2) the high efficiency of gas-phase reactions R21: $CHF_x + F \rightarrow CF_x + HF$, R22: $CHF_x + H \rightarrow CHF_{x-1} + HF$ and R23: $CF_x + H \rightarrow CF_{x-1} + HF$. Accordingly, main formation channels for F atoms are R24: $HF + e \rightarrow H + F + e$ and R5 for x = 2, 3. Another important feature is that the contribution of R21 to the total decay rate for F atoms exceeds those for R6 and R7. The substitution of Ar for O_2 retards the electron-impact dissociation kinetics (because of sufficient falls in both T_e and n_e) as well as strongly suppresses all F atom formation pathways which do work in the CHF_3 + Ar plasma. The last effect

is caused by a) fast losses of CF_x and CHF_x radicals due to their effective conversion into CF_xO species in R8, R25: $CHF_x + O \rightarrow CF_xO + H$ and R26: $CHF_x + O \rightarrow$ $\rightarrow CF_{x-1}O + HF$; and b) the decreasing rate of R24 due to the tenfold fall in $k_{24}n_e$ (88.5–8.3 s^{-1} at 0–50% O_2). Another remarkable differences in respect to previous gas system are the lower production rates for O and $O(^1D)$ in R27: $O_2 + e \rightarrow 2O + e$ and R28: $O_2 + e \rightarrow$ $\rightarrow O + O(^1D) + e$ as well as the faster decay of oxygen atoms R8, R25 and R26. In fact, this limits the formation of CF_xO and FO species in both gas-phase and heterogeneous reactions and thus, lowers contributions of R11–R13 and R17–R19 to the F atom formation kinetics. All these result in a monotonic decrease in the total F atom formation rate toward O_2-rich plasmas (by ~ 2.3 times at 0-50% O_2). At the same time, rapidly decreasing densities of CHF_x and CF_x radicals reduce the effective decay frequency for F atoms in both heterogeneous (R6, R7) and gas-phase (R21) reactions. Since the last tendency appears to be faster compared with a change in the fluorine atom formation rate, the monotonic increase in [F] takes place (Fig. 1(b)).

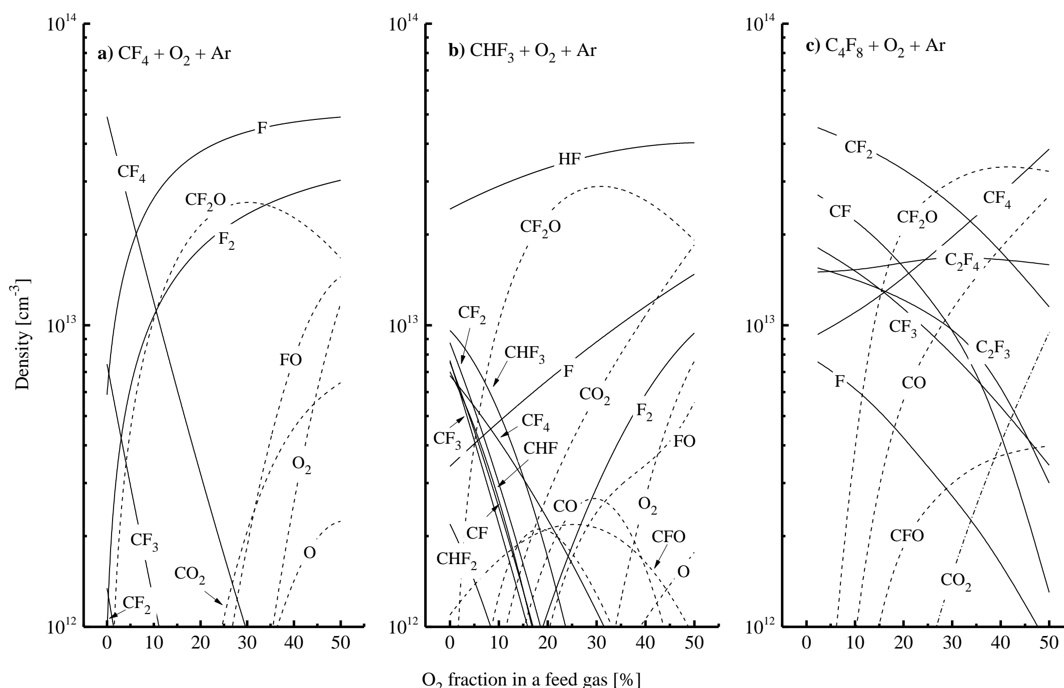

Fig. 1. Steady-state densities of neutral species in $CF_4 + O_2 + Ar$ (a), $CHF_3 + O_2 + Ar$ (b) and $C_4F_8 + O_2 + Ar$ (c) plasmas. Dashed lines indicate the oxygen-containing components

Рис. 1. Стационарные концентрации нейтральных частиц в плазме $CF_4 + O_2 + Ar$ (a), $CHF_3 + O_2 + Ar$ (b) and $C_4F_8 + O_2 + Ar$ (c). Пунктирными линиями выделены кислородсодержащие компоненты

In the $C_4F_8 + Ar$ plasma, the gas phase is mostly composed by fluorocarbon components CF_x (x = 1, 2, 3) and C_2F_x (x = 3, 4) (Fig. 1(c)) [12-14]. These particles appear as the first-step dissociation products of original C_4F_8 molecules in R29: $C_4F_8 + e \rightarrow$ $\rightarrow 2C_2F_4 + e$ and R30: $C_4F_8 + e \rightarrow C_3F_6 + CF_2 + e$ as well as result from the further decomposition of corresponding reaction products through R5 for x = 2, R31: $C_3F_6 + e \rightarrow C_2F_4 + CF_2 + e$, R32: $C_2F_4 + e \rightarrow 2CF_2 + e$ and R33: $C_2F_4 + e \rightarrow C_2F_3 + F + e$. The main source of F atoms is given by R5 for x = 1–3 while their decay in addition to R6 and R7 is noticeably contributed by R34: $C_2F_4 + F \rightarrow CF_2 + CF_3$. The substitution of Ar for O_2 also reduces the efficiency of R5 (due to the simultaneous decrease in T_e and n_e) as well as introduces new pathways for the decomposition of CF_x radicals in a form of R8–R10. At the same time, a decrease in $[CF_x]$ appears to be much slower compared with CF_4- and CHF_3-based plasmas. The reason is the effective loss of O_2 molecules in R35: $CF + O_2 \rightarrow CFO + O$ and R36: $C + O_2 \rightarrow CO + O$ that limits formation rates for O and $O(^1D)$ atoms through R27 and R28. The lack of oxygen atoms reduces the significance of R8, R11–R13 and R17–R19 in respect to production of F atoms while the total F atom formation rate exhibit the monotonic decrease toward O_2-rich plasmas. Accordingly, the same behavior is also for the F atoms density, as shown in Fig. 1(c).

In order to understand how above differences in gas-phase plasma characteristics do influence the reactive-ion etching kinetics, one can use the phenomenological approach developed in earlier works [7, 8,

10, 11]. The latter is based on several experimental studies [22–26] and may be formulated as follows:

- The rate of physical sputtering R_{phys} for both target surface and fluorocarbon polymer film may be expressed as $Y_S\Gamma_+$, where Y_S is the process yield, and $\Gamma_+ \approx J_+/e$ is the ion flux. When taking in mind that $Y_S \sim (M_i\varepsilon_i)^{1/2}$ for the given ion mass, the efficiency of the physical etching pathway in different gas systems with $M_i \approx$ const may be compared using the the parameter $\varepsilon_i^{1/2}\Gamma_+$.

- The rate of chemical reaction R_{chem} between F atoms and target surface may be expressed as $\gamma_R\Gamma_F$, where Γ_F is the flux of F atoms with the gas-phase density [F], and γ_R is the effective reaction probability. The similar formula works also for the chemical interaction of O atoms with polymer surface. The sufficient difference between these two cases is that the reaction of F atoms appears on the polymer/etched surfaced interface and may have the ion-assisted nature. That is why the corresponding γ_R may depend not only on surface temperature, but be also sensitive to any factor influencing the access of etchant species to desorption sites. In general, these are the ion bombardment intensity and the polymer film thickness.

- The growth of polymer film is provided by CH_xF_y ($x + y \leq 2$) radicals as well as appears to be slower in fluorine-rich plasmas. As such, the polymer deposition rate is characterized by the Γ_{pol}/Γ_F ratio, where Γ_{pol} is the total flux of polymerizing radicals, while the change in fluorocarbon polymer film thickness due to physical and chemical decomposition pathways may be traced by parameters $\Gamma_{pol}/\varepsilon_i^{1/2}\Gamma_+\Gamma_F$ and $\Gamma_{pol}/\Gamma_O\Gamma_F$, respectively.

Data of Figs. 1, 2 and 3 allow one to summarize features which may influence heterogeneous process kinetics in given gas systems. First, the substitution of Ar for O_2 in all there gas mixtures introduces identical gas-phase reaction mechanisms to reduce densities of polymerizing radicals, but has specific impacts on the formation-decay balance for F atoms. As a result, an increase in $y(O_2)$ up to 50% does not change the basic rule concerning the correlation between the polymerizing ability and the z/x ratio in original $C_xH_yF_z$ molecules, but disturbs the difference in F atom densities compared with non-oxygenated binary mixtures with Ar [16]. Particularly, the rapid fall of both [F] and Γ_F in the $C_4F_8 + O_2 + Ar$ plasma produces the more than 10 times gap compared with the CF_4 - based gas system as well as leads to lowest values of these parameters among other O_2-rich mixtures. Another principal effect is that even the formally similar changes of F atom density in $CF_4 + O_2 + Ar$ and $CHF_3 + O_2 + Ar$ plasmas are caused by different reasons. These are changes in F atom formation or decay kinetics, respectively. Second, the substitution of Ar for O_2 always suppresses the polymer deposition rate through increasing gap between densities of F atoms and polymerizing radicals. The stronger effect for $CF_4 + O_2 + Ar$ and $CHF_3 + O_2 + Ar$ plasmas (see Fig. 2(b)) is because of increasing density of F atoms and opposite changes in Γ_{pol} and Γ_{pol} toward higher $y(O_2)$ values.

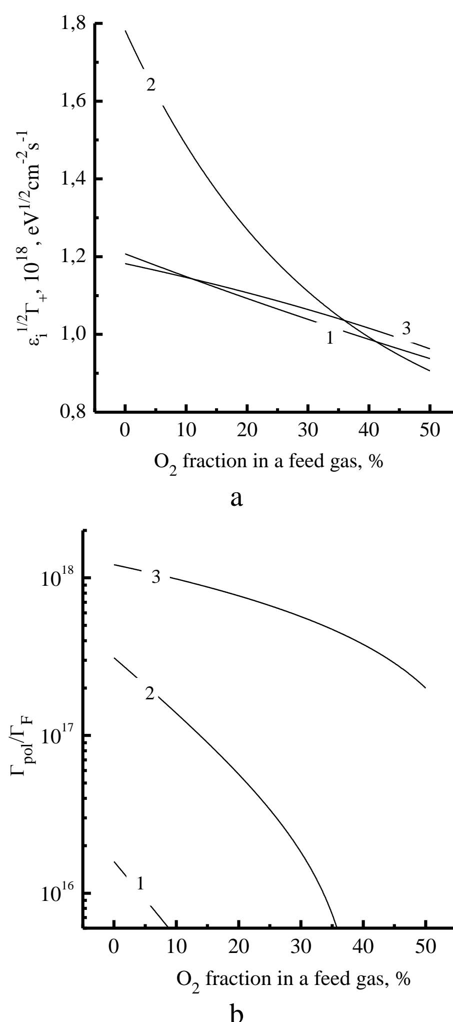

Fig. 2. Gas-phase-related parameters characterizing the ion bombardment intensity (a) and the polymer deposition rate (b) in $CF_4 + O_2 + Ar$ (1), $CHF_3 + O_2 + Ar$ (2) and $C_4F_8 + O_2 + Ar$ (3) plasmas

Рис. 2. Параметры газовой фазы, характеризующие интенсивность ионной бомбардировки поверхности (a) и скорость осаждения полимера (b) в плазме $CF_4 + O_2 + Ar$ (1), $CHF_3 + O_2 + Ar$ (2) и $C_4F_8 + O_2 + Ar$ (3)

And thirdly, the substitution of Ar for O_2 in all three gas systems results in decreasing polymer film thickness. Again, the stronger change of h_{pol} for $CF_4 + O_2 + Ar$ and $CHF_3 + O_2 + Ar$ plasmas is due to the simultaneous acceleration in physical (Fig. 3(a)) and chemical (Fig. 3(b)) polymer decomposition pathways.

In the $C_4F_8 + O_2 + Ar$ plasma, the decrease in $\varepsilon_i^{1/2}\Gamma_+$ (Fig. 2(a)) has almost the same slope with the change in Γ_{pol}/Γ_F ratio (Fig. 2(a)). Such situation causes the nearly constant efficiency for sputter etching of polymer film in the range of 0-50% O_2.

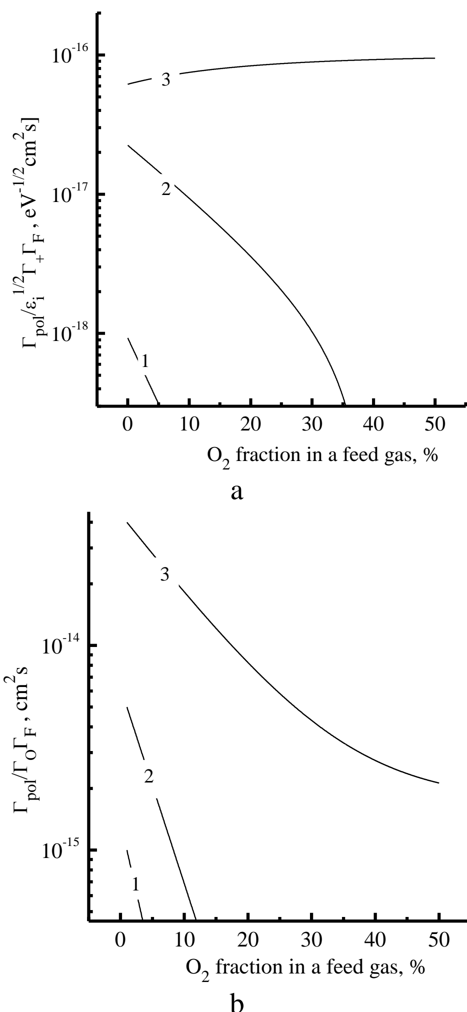

Fig. 3. Gas-phase-related parameters characterizing the change in polymer film thickness due to physical (a) and chemical (b) etching pathways in $CF_4 + O_2 + Ar$ (1), $CHF_3 + O_2 + Ar$ (2) and $C_4F_8 + O_2 + Ar$ (3) plasmas

Рис. 3. Параметры газовой фазы, характеризующие изменение толщины полимерной пленки за счет физического (а) и химического (б) механизмов травления в плазме $CF_4 + O_2 + Ar$ (1), $CHF_3 + O_2 + Ar$ (2) и $C_4F_8 + O_2 + Ar$ (3)

From above data, it can be suggested that the $C_4F_8 + O_2 + Ar$ gas system under the condition of y(O_2) > y(Ar) represents the worse source of etchant species as well as is featured by highest polymer deposition rate and polymer film thickness. Therefore, one can expect the lowest silicon etching rate together with an advanced etching profile. The latter is due to both weaker spontaneous etching (because of lower Γ_F/Γ_+ ratio) and better passivation of sidewalls.

CONCLUSIONS

In this work, we investigated how the O_2/Ar ratio in $CF_4 + O_2 + Ar$, $CHF_3 + O_2 + Ar$ and $C_4F_8 + O_2 + Ar$ gas mixtures does influence plasma parameters and steady-state gas phase compositions under the condition of 13.56 MHz inductive RF discharge. It was shown that the transition toward O_2-rich plasmas a) causes similar changes in electrons- and ions-related plasma parameters (electron temperature, plasma density, ion bombardment energy); b) always suppresses densities of polymerizing radicals and reduces the polymer film thickness; and c) has the different impact on the F atom kinetics. As a result, the presence of oxygen does not disturb the correlation between the polymerizing ability and the z/x ratio in original $C_xH_yF_z$ molecules while the increasing F atom density in the sequence of C_4F_8 - CHF_3 - CF_4 in at 50% O_2 contradicts with that for non-oxygenated plasmas.

The publication was carried out within the framework of the state assignment of the Federal State Institution «Scientific Research Institute for System Analysis of the Russian Academy of Sciences» (fundamental research) on subject No. 0580-2021-0006 “Fundamental and applied research in the field of lithography limits in semiconductor technologies as well as physical and chemical etching processes for 3D nanometer dielectric structures for the development of critical technologies for the production of ECB. Investigations and developments of both models and constructions for microelectronic elements in the extended temperature range (from -60C to +300C)”.

Публикация выполнена в рамках государственного задания ФГУ ФНЦ НИИСИ РАН (проведение фундаментальных научных исследований) по теме № 0580-2021-0006 «Фундаментальные и прикладные исследования в области литографических пределов полупроводниковых технологий и физико-химических процессов травления 3D нанометровых диэлектрических структур для развития критических технологий производства ЭКБ. Исследование и построение моделей и конструкций элементов микроэлектроники в расширенном диапазоне температур (от -60С до +300С)».

REFERENCES
ЛИТЕРАТУРА

1. **Donnelly V.M., Kornblit A.** Plasma etching: Yesterday, today, and tomorrow. *J. Vac. Sci. Technol.* 2013. V. 31. P. 050825-48. DOI: 10.1116/1.4819316
2. **Nojiri K.** Dry etching tech.nology for semiconductors. Tokyo: Springer Internat. Publ. 2015. 116 p. DOI: 10.1007/978-3-319-10295-5.
3. Advanced plasma processing technology. New York: John Wiley & Sons Inc. 2008. 479 p.

4. **Lieberman M.A., Lichtenberg A.J.** Principles of plasma discharges and materials processing. New York: John Wiley & Sons Inc. 2005. 757 p. DOI: 10.1002/0471724254.
5. **Kimura T., Noto M.** Experimental study and global model of inductively coupled CF_4/O_2 discharges. *J. Appl. Phys.* 2006. V. 100. P. 063303-12. DOI: 10.1063/1.2345461.
6. **Kimura T., Ohe K.** Probe measurements and global model of inductively coupled Ar/CF_4 discharges. *Plasma Sources Sci. Technol.* 1999. V. 8. P. 553-560. DOI: 10.1088/0963-0252/8/4/305.
7. **Chun I., Efremov A., Yeom G. Y., Kwon K.-H.** A comparative study of $CF_4/O_2/Ar$ and $C_4F_8/O_2/Ar$ plasmas for dry etching applications. *Thin Solid Films.* 2015. V. 579. P. 136-143. DOI: 10.1016/j.tsf.2015.02.060.
8. **Efremov A., Lee J., Kim J.** On the Control of Plasma Parameters and Active Species Kinetics in $CF_4 + O_2 + Ar$ Gas Mixture by CF_4/O_2 and O_2/Ar Mixing Ratios. *Plasma Chem. Plasma Proc.* 2017. V. 37. P. 1445-1462. DOI: 0.1007/s11090-017-9820-z.
9. **Ho P., Johannes J.E., Buss R.J.** Modeling the plasma chemistry of C_2F_6 and CHF_3 etching of silicon dioxide, with comparisons to etch rate and diagnostic data. *J. Vac. Sci. Technol. B.* 2001. V. 19. P. 2344-2367. DOI: 10.1116/1.1387048.
10. **Efremov A.M., Murin D.B., Kwon K.H.** Parameters of plasma and kinetics of active particles in $CF_4(CHF_3)$ + Ar mixtures of a variable initial composition. *Russ. Microelectronics*. 2018. V. 47. N 6. P. 371-380. DOI: 10.1134/S1063739718060033.
11. **Efremov A.M., Murin D.B., Kwon K.H.** Plasma Parameters and Kinetics of Active Particles in the Mixture $CHF_3 + O_2$ + Ar. *Russ. Microelectronics.* 2020. V. 49. N 4. P. 233-243. DOI: 10.1134/S1063739720030038.
12. **Kokkoris G., Goodyear A., Cooke M., Gogolides E.** A global model for C_4F_8 plasmas coupling gas phase and wall surface reaction kinetics. *J. Phys. D. Appl. Phys.* 2008. 41. P. 195211-23. DOI: 10.1088/0022-3727/41/19/195211.
13. **Rauf S., Ventzek P.L.** Model for an inductively coupled Ar/c-C_4F_8 plasma discharge. *J. Vac. Sci. Technol. A.* 2002. V. 20. P. 14-23. DOI: 10.1116/1.1417538.
14. **Ефремов А.М., Мурин Д.Б., Квон К.Х.** Параметры плазмы, концентрации активных частиц и кинетика травления в смеси C_4F_8+Ar. *Изв. вузов. Химия и хим. технология.* 2019. Т. 62. Вып. 2. С. 31–37
Efremov A., Murin D., Kwon K.-H. Plasma parameters, densities of active species and etching kinetics in C_4F_8+Ar gas mixture. *ChemChemTech [Izv. Vyssh. Uchebn. Zaved. Khim. Khim. Tekhnol.].* 2019. V. 62. N 2. P. 31-37. DOI: 10.6060/ivkkt.20196202.5791.
15. **Lee B. J., Efremov A., Nam Y., Kwon K.-H.** Plasma Parameters and Silicon Etching Kinetics in $C_4F_8 + O_2$ + Ar Gas Mixture: Effect of Component Mixing Ratios. *Plasma Chem. Plasma Process*. 2020. V. 40. P. 1365-1380. DOI: 10.1007/s11090-020-10097-9.
16. **Efremov A., Murin D., Kwon K.-H.** Concerning the Effect of Type of Fluorocarbon Gas on the Output Characteristics of the Reactive-Ion Etching Process. *Russ. Microelectronics.* 2020. V. 49. N 3. P. 157-165. DOI: 10.1134/S1063739720020031.
17. **Shun'ko E.V.** Langmuir probe in theory and practice. Boca Raton: Universal Publ. 2008. 245 p.
18. **Efremov A., Lee J., Kwon K.-H.** A comparative study of CF_4, Cl_2 and HBr + Ar Inductively Coupled Plasmas for Dry Etching Applications. *Thin Solid Films.* 2017. 629. P. 39-48. DOI: 10.1016/j.tsf.2017.03.035.
19. **Hsu C.C., Nierode M.A., Coburn J.W., Graves D.B.** Comparison of model and experiment for Ar, Ar/O_2 and $Ar/O_2/Cl_2$ inductively coupled plasmas. *J. Phys. D Appl. Phys.* 2006. V. 39. N 15. P. 3272-3284. DOI: 10.1088/0022-3727/39/15/009.
20. **Proshina O., Rakhimova T.V., Zotovich A., Lopaev D.V., Zyryanov S.M., Rakhimov A.T.** Multifold study of volume plasma chemistry in Ar/CF_4 and Ar/CHF_3 CCP discharges. *Plasma Sources Sci. Technol.* 2017. V. 26. P. 075005. DOI: 10.1088/1361-6595/aa72c9.
21. **Takahashi K., Hori M., Goto T.** Characteristics of fluorocarbon radicals and CHF_3 molecule in CHF_3 electron cyclotron resonance downstream plasma. *Jpn. J. Appl. Phys.* 1994. V. 33. P. 4745-4758. DOI: 10.1143/JJAP.33.4745.
22. **Gray D.C., Tepermeister I., Sawin H.H.** Phenomenological modeling of ion-enhanced surface kinetics in fluorine-based plasma-etching. *J. Vac. Sci. Technol. B.* 1993. V. 11. P. 1243-1257. DOI: 10.1116/1.586925.
23. **Standaert T.E.F.M., Hedlund C., Joseph E.A., Oehrlein G.S., Dalton T.J.** Role of fluorocarbon film formation in the etching of silicon, silicon dioxide, silicon nitride, and amorphous hydrogenated silicon carbide. *J. Vac. Sci. Technol. A.* 2004. V. 22. P. 53-60. DOI: 10.1116/1.1626642.
24. **Schaepkens M., Standaert T.E.F.M., Rueger N.R., Sebel P.G.M., Oehrlein G.S., Cook J.** Study of the SiO_2-to-Si_3N_4 etch selectivity mechanism in inductively coupled fluorocarbon plasmas and a comparison with the SiO_2-to-Si mechanism. *J. Vac. Sci. Technol. A.* 1999. V. 17. P. 26-37. DOI: 10.1116/1.582108.
25. **Matsui M., Tatsumi T., Sekine M.** Relationship of etch reaction and reactive species flux in $C_4F_8/Ar/O_2$ plasma for SiO_2 selective etching over Si and Si_3N_4. *J. Vac. Sci. Technol. A.* 2001. V. 19. P. 2089-2096. DOI: 10.1116/1.1376709.
26. **Kastenmeier B.E.E., Matsuo P.J., Oehrlein G.S.** Highly selective etching of silicon nitride over silicon and silicon dioxide. *J. Vac. Sci. Technol. A.* 1999. V. 17. P. 3179-3184. DOI: 10.1116/1.582097.

Поступила в редакцию 24.02.2021
Принята к опубликованию 01.04.2021

Received 24.02.2021
Accepted 01.04.2021